# GO-CFAR Trained Neural Network Target Detectors

*Jabran Akhtar and Karl Erik Olsen*
Norwegian Defence Research Establishment (FFI)
Box 25, 2027 Kjeller, Norway
Email: jabran.akhtar@ffi.no, karl-erik.olsen@ffi.no

***Abstract*—Detecting targets embedded in noise and clutter is an essential task for many radar systems. A competent system must additionally offer high probability of detection with a low false alarm rate and a standard practice is to employ constant false alarm rate (CFAR) detectors. In this article, we develop and expand the use of neural networks to accomplish this objective. The neural networks are trained to recognize targets in a specified environment subject to the proposed conditions ascribed by a traditional CFAR detector. We show that after an initial learning process, a trained neural network can offer improved detectional performance. The improvement is related to either a lower false alarm rate or a slightly greater probability of detection.**

Keywords: radar, detection, constant false alarm rate (CFAR), clutter, Swerling targets, neural network

## I. Introduction

One of the core radar tasks has always been to detect fluctuating targets with a high probability of detection ($P_D$) and a low false alarm rate ($P_{FA}$). A typical technique employed for this purpose is the constant false alarm rate (CFAR) detector [1], [2] with several adaptations. The received signal is then evaluated on a cell to cell basis. Each cell is compared against an average composed of select neighboring cells and if the signal value in the test cell exceeds the determined average by a given margin then a detection is declared. A common version of the detector, often applied in clutter environments, is the GO (Greatest Of)-CFAR detector.

CFAR detectors have been studied in great details over the last decades; nevertheless, there generally remains a trade-off between various CFAR techniques, as an improvement in probability of detection often comes at the expense of false alarm rate and vice versa. The last couple of years have also witnessed a large growth in the application of deep learning and neural networks. These networks can be trained to be exceptionally good at classification of signals and images [3], [4]. The use of machine learning has also been studied in radar contexts to perform target detection using different strategies [5], [6], [7], [8], [9], [10], [11]. In [12] the authors proposed an approach to train a neural network where the objective was to return the same type of detectional performance as of cell averaging (CA)-CFAR while otherwise aiming to return a lower false alarm rate. The training and validation was carried out on a simple radar environment consisting of fluctuating targets in noise. The presence of clutter was not considered and it was assumed that the radar only operated on a single pulse mode restricting the applicability of the method. Despite these limitations, the results demonstrated that neural networks have the potential to improve on traditional detection.

This article builds upon the primary idea of [12] to introduce a more general training setting. A new method for training of artificial neural networks is also proposed where the network is not restricted to train on binary outcomes from the final layer, rather a more dynamic output ratio is contemplated. Seeking a ratio as the output from a neural network turns out to play an important role in being able to offer a higher probability of detection than CFAR without necessarily increasing the $P_{FA}$. The detection and training procedure is implemented on range-Doppler maps generated by multiple incoming pulses. This provides a generic set for model training and evaluation closely mimicking realistic operational cases. Simulations under various conditions with fluctuating targets with and without the presence of K-distributed clutter are carried out to demonstrate the improvement in performance obtained through trained neural networks assessed against conventional CFAR methods.

## II. System model

To provide a setup for the neural network training and assessment, we model a standard pulsed radar system where a waveform $p(t)$ is transmitted at steady intervals. After transmission of each pulse, the incoming echoes are sampled and a pulse compression is performed through standard matched-filtering,

$$\mathbf{r}(t,u) = p^*(-t) * \ (\sum_n \sigma_n p(t-\Delta_n) e^{j v_{n,u}} + q(t,u) + w(t)), \tag{1}$$

where $t = 1, 2, ..., R$. $t$ is the discrete fast-time parameter corresponding to different time delays (range cells) while $R$ is the maximum radar range. $M$ pulses are emitted in a coherent processing interval (CPI), $u = 1, ..., M$ (slow-time), and in the arriving echoes $\sigma_n$ and $\Delta_n$ point to, respectively, the reflectivity and the delay of reflector $n$. $j = \sqrt{-1}$ and $e^{j v_{n,u}}$ is the Doppler shift for each target which for a fixed pace object can be described by

$$v_{n,u} = v_{n,u-1} + \frac{\theta_n \ 4\pi f_c}{c \ \text{PRF}}, \ \ u = 1, ..., M \tag{2}$$

assuming $v_{n,0} = 0$ and $\theta_n$ being the radial velocity of target $n$, PRF the pulse repetition frequency, $f_c$ the radar carrier frequency and $c$ propagation velocity [2]. In (1), $q(t,u)$ is the contribution from clutter in the received signal while $*$ specifies convolution and $w(t)$ is white Gaussian noise. The targets are presumed to be slowly fluctuating with Swerling 1 distribution where $\sigma_n$ varies randomly from CPI to CPI but with a mean signal-to-noise ratio (SNR). After gathering all pulses, the slow-time domain of $\mathbf{r}(t,u)$ is multiplied by a windowing function $\mathbf{w}$ and thereupon Fourier transformed to yield a range-Doppler map:

$$\mathbf{d}(t,\omega) = \mathbf{F} \ \mathbf{w} \ \mathbf{r}(t,u), \ \in \mathbb{C}^{M \times R}. \tag{3}$$

978-1-7281-1679-2/19/$31.00 ©2019 IEEE

$\mathbf{F}$ is the discrete Fourier matrix of size $M \times M$, $\mathbf{F}_{k,l} = \exp(-j2\pi kl/M)$. Following Fourier transform, targets with a steady pace will appear concentrated in Doppler while clutter, often with a different velocity characteristic, may show up detached. To locate likely targets, a CFAR detector can be executed on the range-Doppler map.

### A. CFAR detector

A CFAR detector takes the square law range samples of $\hat{\mathbf{d}}(t,\omega) = |\mathbf{d}(t,\omega)|^2 \ \forall \ t,\omega$ and evaluates each single cell to ascertain if detection conditions are satisfied. In this paper, we utilize a standard one dimensional CFAR detector where averaging is conducted across the range domain. A sliding window of size $2N+2G+1$ is chosen and shifted across all possible bins, $\hat{t} = 1+N+G, ..., R-N-G$ and $\omega = 1, ..., M$, excluding potential edges. The $2N+2G+1$ samples in range are extracted in $x(u) = \hat{\mathbf{d}}(\hat{t}-N-G : \hat{t}+N+G, \omega),\ u = 1, 2, ..., 2N+2G+1$ and the cell in the middle of the window, $x(N+G+1)$ cell under test (CUT), is compared against an average. $G$ number of guard cells to the right and left of CUT are neglected. The average, $\gamma$, in GO cell averaging is estimated as the maximum average of the $N$ cells to the left or to the right,

$$\gamma = \frac{1}{N}\ \max\ (\ \sum_{k=1}^{N} x(k), \sum_{k=N+2G+2}^{2N+2G+1} x(k)\ ). \tag{4}$$

A detection occurs if

$$x(u)_{|u=CUT} > \gamma\ K, \tag{5}$$

where $K$ (dB) is a set threshold.

### B. Detection with a neural network

The GO-CFAR process is an established mechanism for extracting targets in clutter and noise. This process would therefore need to be transferred into a neural network offering a comparable behavior but with an improved overall performance. The effectiveness of neural networks depends strongly on training and the available quantity of learning data. The learning process can accordingly be constructed on collected or simulated radar data where one is informed of the exact target positions. What we propose are training strategies where conventional CFAR detectors mutually aid in the process to differentiate out targets and operate as training instructors.

For the neural network, depicted in figure 1, we assume a setup where the CFAR window is, as previously, shifted across the range-Doppler map, but the window samples, including guard cells, are normalized and then dispensed into a fully-connected feed-forwarding network. The normalization is carried out by min max normalization to adjust the values to the range within 0 to 1, $\hat{x}(t) = \frac{x(t)-\min(x(t))}{\max(x(t))-\min(x(t))}$. We consider the problem of selecting a network size as a secondary issue in regard to this work though the same number of nodes in each layer as the number of CFAR samples and 3 to 4 hidden layers generally present solid results. The output from the last layer, $\kappa$, returns a detection estimate. A threshold value is finally applied on $\kappa$ and if a prescribed value is surpassed then a detection is affirmed.

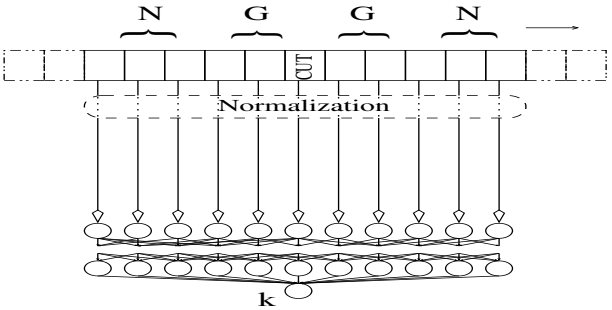


Fig. 1: Neural network detector

Decisive training of a network is essential for it to succeed and for this we assume that $L$ number of independent range-Doppler maps $\mathbf{r}(t,\omega)_1, ...., \mathbf{r}(t)_L$ have been collected wherein the targets and their locations in range and Doppler are precisely known. For each map, the whole image can be used for training, or to lessen the computational load, representative random areas within each map may be selected where the sliding CFAR window is executed. The ares selected should contain the target at a known position, the regions within the proximity of the targets, clutter samples and noise only samples. Further on, if the noise or clutter plane is constant at a set value across all maps then the trained neural network may not adapt well to altering surroundings. The average noise and clutter floors should therefore fluctuate in the training data set. The parameter presumed fixed during training is the threshold value $K$. This regulates the $P_D$ for the standard CFAR algorithm and is the performance objective for the network. Two different training schemes on what the predicted output, $\hat{\kappa}$, from the final layer should be are discussed next.

### C. Training scheme A

This training scheme operates with a binary digit and the predicted output from the network for each block of training data is either 0, in case of no detection; or 1 if a target is found. Explicitly, the last layer trains to yield:

$$\hat{\kappa} = \begin{cases} 1, & \text{a target is at CUT } \textit{and} \\ & \text{GO-CFAR test is positive.} \\ \\ 0, & \text{else.} \end{cases}$$

The positive training correlates with a traditional GO-CFAR method for target detection, notwithstanding equally important is the fact that the network now aims to return a zero in the absence of real targets disregarding the CFAR response. Such a trained neural network should ideally be able to approximate the same type of $P_D$ performance as of the original CFAR method but with a lower $P_{FA}$. This training strategy is related to [12].

### D. Training scheme B

The introductory scheme A is easy to apprehend but it does have one drawback that it can by convention only return a positive outcome if GO-CFAR consents in returning a detection. The GO-CFAR test can fail if the target does singles out but is beneath the detection threshold $K$. A revised technique can therefore attempt to forego a strict bound like

978-1-7281-1679-2/19/$31.00 ©2019 IEEE

this and instead return the CFAR test ratio between CUT and the averaging factor, restricted to the upper value of 1. This should notably only be returned if a true target is known to be at cell under test. The ideal returning value will thus be 1 if a target fulfills the CFAR detection threshold, within 0 and 1 if the target is recognizable but does not obey the CFAR test and 0 is no target is identified. The second training strategy is correspondingly:

$$\hat{\kappa} = \begin{cases} \max\left(1, \frac{x(u)_{|u=CUT}}{\gamma K}\right), & \text{a target is at CUT.} \\ 0, & \text{else.} \end{cases}$$

A detection threshold set on the final layer decides if a detection is to be affirmed. For further elaboration of the schemes we refer to [13].

The training procedure is visualized in figure 2. We emphasize that for both training strategies, the provision "target is present at CUT" must also include neighboring cells if a target stretches out in range or Doppler due to for example sidelobes. The training process will determine appropriate weights for the neural network to minimize the difference between the desired output and the factual network output, $\epsilon = \min \sum |\kappa - \hat{\kappa}|^2$ over all CFAR training blocks. Subsequently training, the final performance can be settled by enacting a much larger untrained data set thorough the network.

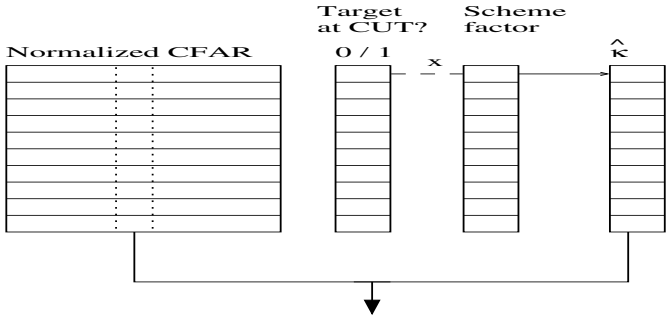


Fig. 2: The training process

## III. Simulation results

A pulsed radar system is modeled and simulated to train neural networks under the presented schemes and then compare the performance against traditional GO-CFAR detection. Multiple targets are simulated in each dwell alongside clutter and noise. The radar is assumed to transmit and receive $M = 16$ pulses over 300 simulated range bins with a resolution of 800m. In total, four independently Swerling 1 fluctuating targets are modeled being placed at range bins 75, 125, 210 and 260 with a random speed.

From the four targets, the first two are modeled as stronger reflectors but also placed in the locality of simulated clutter. The clutter is modeled using K-distribution and encompasses the first half of range bins. The GIT [14] model is used to provide estimates for the clutter reflectivity level with a radar carrier frequency of 3GHz and a radar elevation of 500m. The clutter shape parameter is randomly set for each CPI to be in the range between $v = 0.05$ (spiky) and $v = 10$ (Rayleigh distributed) [14], [15], [16]. Random up or down scaling on the

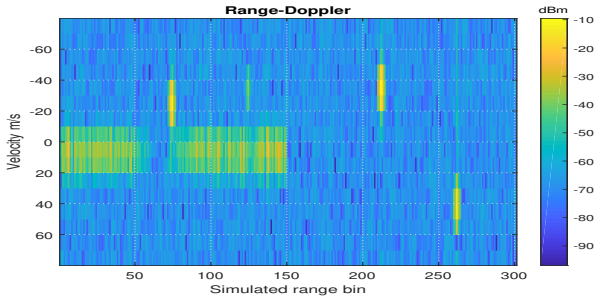


Fig. 3: Example of simulated range-Doppler map

clutter is done to provide more variation in the signal-to-clutter ratios from CPI to CPI. The last two targets are presumed in a noise only region, being placed farther out from the radar; thus their average gain is set lower by a factor of 20dB. Moreover, the noise floor is not kept fixed rather ranges between $-80$ dB to $-115$ dB following a uniform distribution between CPIs. An example of such randomly generated range-Doppler maps (where the targets stand out) is given in figure 3. The dwell to dwell diversity of the above setup, encompasses a wide types of CFAR blocks and should be applicable for training a versatile detector geared towards point targets in clutter and noise.

For generation of range-Doppler maps the Hamming window is applied. After map formation, CFAR tests are performed and the blocks extracted for the training database, the CFAR parameters being set as $G = 3$ guard cells and $N = 6$ averaging cells on each side. To reduce the computational load, the CFAR process was executed over randomly selected 15% of range-Doppler cells, though cells containing targets were always incorporated. The mechanism was iterated for $L = 2000$ independent range-Doppler maps. A complete training set based on the above contained 1.4 million CFAR entries with a total of 40000 probable targets (including Doppler spread entries), from whom 35% were correctly detected by GO-CFAR. The average SNR over all CPIs ranged from $-40$ dB to 75 dB while the signal-to-clutter ratio varied between $-60$ dB to 60 dB. This data was then used to train a fully-connected feed-forwarding network with four hidden layers and 19 nodes in each layer with *tanh* as the node activity function. Scale conjugate gradient algorithm was applied for a maximum of 20000 epochs.

Following training, a 50 times bigger set of range-Doppler images was generated under the same simulated conditions but now with a set mean power value for the targets. Each resulting map was completely evaluated through both GO-CFAR and the trained neural network. This procedure was repeated with differing average target power levels to attain $P_D$ and $P_{FA}$ curves with respect to mean target signal-to-clutter plus noise ratio (SCNR). $P_D$ was calculated as the number of correctly detected targets relative to the total number of simulated targets while $P_{FA}$ as the number of incorrectly detected targets in relation to correctly detected targets. For the described simulations, the main detection thresholds utilized are $\kappa > 0.5$ and $\kappa > 0.8$.

Figures 4 and 5, respectively, display $P_D$ (left) and $P_{FA}$ (right) curves generated through the described simulation con-

978-1-7281-1679-2/19/$31.00 ©2019 IEEE

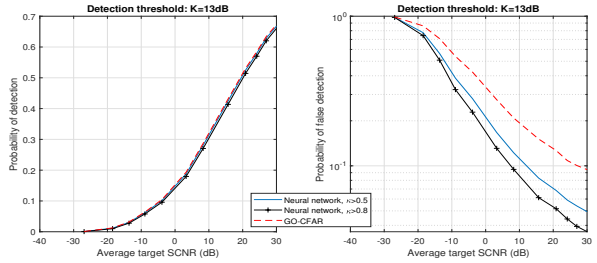


Fig. 4: Scheme A: $P_D$ and $P_{FA}$

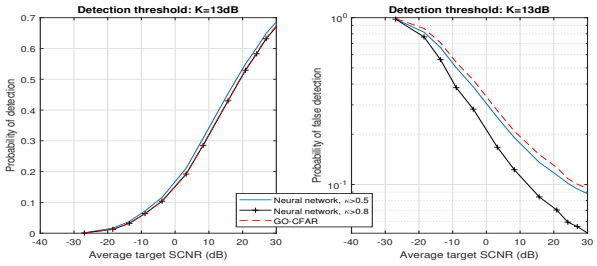


Fig. 5: Scheme B: $P_D$ and $P_{FA}$

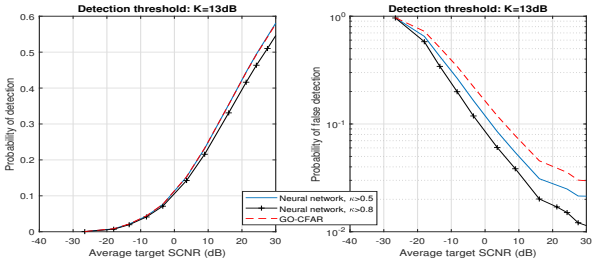


Fig. 6: Scheme A: $P_D$ and $P_{FA}$

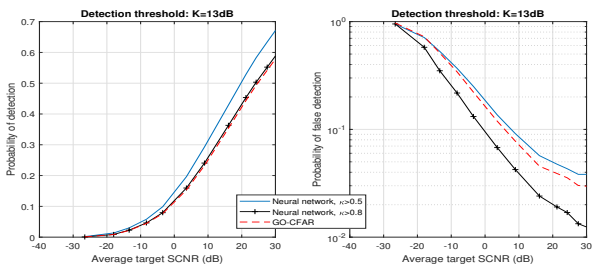


Fig. 7: Scheme B: $P_D$ and $P_{FA}$

ditions under the relative low threshold of $K = 13$ dB for schemes A and B. We point out that the scenario follows the same previous arrangements and the noise and clutter floor still vary from CPI to CPI. The x-axis therefore only provides the average SCNR in dB which would be the average of target power and the average noise and clutter level over a broad range of CPIs.

From figure 4 the probability of detection in Scheme A mirrors the curve of GO-CFAR given in red dashed line. The disparity between the curves is minor, a threshold of $0.5$ gives a similar contour compared to GO-CFAR while the difference increases a bit if the threshold is set to $0.8$. In both cases, the neural network manages to reproduce the GO-CFAR $P_D$ performance with a slight loss. However, scrutinizing the $P_{FA}$ plot on the right side then there is a marked difference between the outcomes from the neural network and GO-CFAR. The neural network detector succeeds in lowering the false alarm rate substantially.

The outcomes from training under scheme B are in figure 5. The $P_D$ exhibits the same form as of GO-CFAR, but it is no longer bounded by the CFAR curve. For a high threshold of $0.8$ it closely follows GO-CFAR but with a threshold of $0.5$ offers a little improvement in detection probability. This comes at an expense of $P_{FA}$ which is higher than scheme A but in both threshold cases manages to outdo CFAR. For this type of scenario and for the selected parameters, scheme B with a threshold of $0.5$ improves modestly upon CFAR on both ends.

The network training and simulations were subsequently reproduced on a different type of scenario with an adjusted set of target parameters. In the modified scenario, each target covered an extra adjoining range cell with a random probability of 0.5. If true, the neighboring cell followed the same power distribution but with an independent value. On top of that, two sidelobes over two adjacent cells of $-20$dB and $-26$dB were added to each of the target cells. This models multiple adjoining targets or a large target with several independent reflectors. The number of guard cells was increased to $G = 4$ while the averaging cells increased to $N = 10$, the neural network thus contained 29 nodes in four hidden layers. Figures 6 and 7 show the results under the new constrains. As previously, method A restricts the improvement in probability of detection which is therefore on level with GO-CFAR while the $P_{FA}$ is marginally better for $\kappa > 0.5$. This provides a good enhancement for the threshold value of $0.5$ if the CFAR $P_D$ is to be retained. In scheme B, the improvement in $P_D$ is clear while the $P_{FA}$ is also noticeable lower for detection threshold of $0.8$ while at $0.5$ is higher than traditional GO-CFAR. By setting the node threshold at $0.8$ this network would give a CFAR comparable $P_D$ but with a lower $P_{FA}$.

The performance results above originate from the training and evaluation based on the designated scenarios and the conditions imposed upon targets, clutter and noise. The last setting is intended to be a rather generic one and to demonstrate that this is indeed the case the trained neural networks were tested on a different type of simulated setup selected from [12] where the transmission and reception of a single pulse takes place and upon which a CFAR process is executed. For this model, only two Swerling 1 fluctuating targets with two range sidelobes are simulated alongside variable Gaussian noise. In these simulations, the SNR ranged from $-100$ to $50$ dB while the noise floor fluctuated between $-70$ to $-35$ dB. The composition of this gives a system where the target power levels and noise floor exhibit a very different characteristic compared to the earlier models engaged in this text.

The resulting plots are provided in figures 8 and 9, obtained by running the neural networks corresponding to figures 4 to 5. In these noise only cases, there is progressive improvement in $P_D$ from scheme A to scheme B while simultaneously an equivalent degradation in $P_{FA}$ with the threshold value of $0.5$. The threshold value of $0.8$, in all cases, gives a sharply lower

978-1-7281-1679-2/19/$31.00 ©2019 IEEE

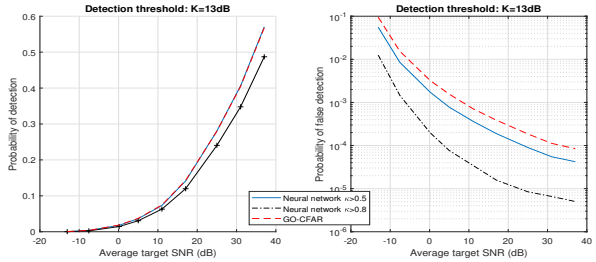


Fig. 8: Scheme A, noise only scenario: $P_D$ and $P_{FA}$

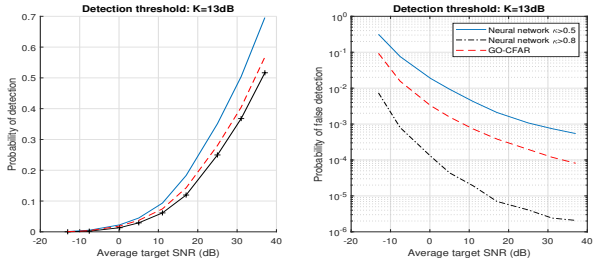


Fig. 9: Scheme B, noise only scenario: $P_D$ and $P_{FA}$

$P_{FA}$ but can in fact still return roughly the same probability of detection as of GO-CFAR using scheme B. The false alarm rate, defined as the number of false detections relative to the total number of tests, is also provided for comparison in figure 10. In the absence of clutter, both scheme A and B are able to yield a consistent alarm rate regardless the SNR. These results confirm the previous conclusions and illustrate the adaptability of well-trained networks.

## IV. Conclusion

This article considered trained artificial neural networks as replacement for conventional CFAR detectors. Training schemes were proposed on how to train such networks to augment on probability of detection and / or reduction in false alarms. All of these techniques relied strongly on standard CFAR to establish the output from the trained neural network. Simulations carried out with fluctuating targets incorporating K-distributed clutter and noise were used for training and evaluation. The outcomes demonstrate that, at least for specifically trained scenarios, the performance of a traditional CFAR detector can be improved significantly by trained artificial neural networks.

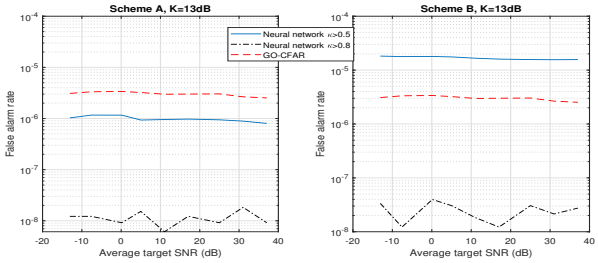


Fig. 10: False alarm rates, noise only scenario

## References


[1] P. P. Gandhi and S. Kassam, "Analysis of CFAR processors in non-homogeneous background," *IEEE Aerospace and Electronic Systems Magazine*, vol. 24, no. 4, pp. 427–445, July 1988.

[2] W. L. Melvin and J. A. S. (Eds.), *Principles of Modern Radar*. SciTech Publishing, 2013.

[3] R. Reed and R. J. Marks, *"Neural Smithing, Supervised Learning in Feedforward Artificial Neural Networks"*. MIT Press, 1999.

[4] C. M. Bishop, *"Pattern Recognition and Machine Learning"*. Springer, 2006.

[5] F. Amoozegar and M. Sundareshan, "A robust neural network scheme for constant false alarm rate processing for target detection in clutter environment," in *Proc. American Control Conference*, 1994.

[6] P. P. Gandhi and V. Ramamurti, "Neural networks for signal detection in non-gaussian noise," *IEEE Trans. Signal Processing*, vol. 45, no. 11, pp. 2846–2851, Nov. 1997.

[7] N. Galvez, J. Pasciaroni, O. Agamennoni, and J. Cousseau, "Radar signal detector implemented with artificial neural networks," in *Proc. XIX Congreso Argentino de Control Automatico*, 2004.

[8] K. Cheikh and F. Soltani, "Application of neural networks to radar signal detection in K-distributed clutter," *IET Radar, Sonar & Navigation*, vol. 153, no. 5, pp. 460–466, Oct. 2006.

[9] D. Mata-Moya, N. del Rey-Maestre, V. Peláez-Sánchez, M.-P. Jarabo-Amores, and J. M. de Nicolás, "MLP-CFAR for improving coherent radar detectors robustness in variable scenarios," *Elsevier Expert Systems with Applications*, vol. 42, no. 11, pp. 4878–4891, July 2015.

[10] B. Rohman, D. Kurniawan, and M. Miftahushudur, "Switching CA/OS CFAR using neural network for radar target detection in non-homogeneous environment," in *Proc. International Electronics Symposium*, 2015.

[11] S. Wunsch, J. Fink, and F. K. Jondral, "Improved detection by peak shape recognition using artificial neural networks," in *Proc. VTC Fall*, 2015.

[12] J. Akhtar and K. E. Olsen, "A neural network target detector with partial CA-CFAR supervised training," in *Proc. of International Conference on Radar*, 2018.

[13] ——, "Training of neural network target detectors mentored by CFAR," *IEEE Trans. Aerospace and Electronic Systems*, in review 2019.

[14] M. M. Horst, F. B. Dyer, and M. Tuley, "Radar sea clutter model," in *Proc. of the Intl. IEEE AP/S URSI Symposium*, 1978, pp. 6–10.

[15] I. Antipov, "Analysis of sea clutter data," in *Defence Science and Technology (DSTO), Australia, Techical Report DSTO-TR-0647*, 1998.

[16] K. Ward and R. Tough, "Radar detection performance in sea clutter with discrete spikes," in *Proc. of Intl. Radar Conference*, 2002.


978-1-7281-1679-2/19/$31.00 ©2019 IEEE